Semiconductor Physics, Quantum Electronics & Optoelectronics, 2013. V. 16, N 4. P. 382-386.

PACS 61.80.Fe

Effect of 1.9-MeV electron irradiation on characteristics of reactively-pressed TiB_2–TiC ceramic composites

I.N. Totsky[1], A.Yu. Popov[2], V.A. Makara[2]

[1]*Taras Shevchenko Kyiv National University, Department of Physics, 2/1, Academician Glushkov Ave., 03680 Kyiv, Ukraine*

[2]*Training-and-Research Center "Physico-Chemical Materials Science" of the Taras Shevchenko Kyiv National University and National Academy of Sciences of Ukraine, 64, Volodymys'ka str., 01033 Kyiv, Ukraine; e-mail: all_popov@bigmir.net*

Abstract. Considered in this paper is the effect of electron irradiation on the phase-structural state and micromechanical characteristics of reactively- and nonreactively-pressed TiB_2–TiC composite ceramic materials. It is shown that reactively-pressed specimens after irradiation demonstrate a growing tendency to phase formation, which considerably affects proceeding of relaxation processes in them. This special feature of reactively-pressed ceramics can improve radiation resistance of construction materials.

Keywords ceramics, electron irradiation, mechanical properties, reactive hot pressing.

Manuscript received 23.07.13; revised version received 12.09.13; accepted for publication 23.10.13; published online 16.12.13.

1. Introduction

Using the procedure of reactive hot pressing with the reaction

$2MeC + B_4C \rightarrow 2MeB_2 + 3C$

(Me stands for Ti, Zr or Hf), one can obtain compact micro- and nanograin materials without pregrinding initial powders, as well as reduce duration, temperature and pressure of hot pressing [1-4]. As a result, the cost price of synthesized materials is considerably reduced. By choosing the appropriate parameters of reactive hot pressing, it is possible to obtain non-equilibrium material owing to incompleteness of the reaction process.

In addition, formation of nuclei of new phases in the course of blend compaction leads to appearance of many submicron grains in the material and, as a result, to a considerable surface energy. Taking all the above-mentioned into account, the reactively-pressed materials may have some energy content. This may affect the character of structural-phase transformations being subjected to irradiation.

According to the Seitz theory for relativistic electrons, the critical energy of defect-forming electron (E_{oc}) can be obtained from the expression [5]:

$$T = \frac{E_0\left(E_0 + 2mc^2\right)}{Mc^2}. \qquad (1)$$

Here, T is the maximal energy transmitted by electron to a target atom in the course of scattering, E_0 – energy of incident electron, m(M) – mass of electron (target atom). To produce a defect in a crystal lattice, it is necessary to transmit to an atom the energy above E_d (25 eV). By inserting that value for T to Eq. (1), we obtain that E_{oc} is close to 0.25 MeV for B and C atoms and close to 1 MeV for Ti atom. Thus, in the case of the incident electron energy below E_{oc}, most of the energy is transmitted to the atomic system without defect production. This energy may be spent for target heating or structural-phase transformations. The latter may promote partial relaxation of the stresses related to accumulation of radiation defects.

Taking into account the possibility of application of hafnium carbide as a reactive component under reactive hot pressing, one can conclude that investigation of features of the irradiation effect on structural-phase transformations in reactively-pressed composites can help to increase in the radiation resistance of HfB_2-containing materials.

In this work, we have studied a possibility in principle to activate structural-phase transformations under the action of electron irradiation and the effect of these transformations on the mechanical characteristics of ceramic materials.

2. Materials and exploratory procedure

We considered distinctions in behavior of mechanical characteristics of TiB_2–TiC-based composites synthesized in different ways and subjected to 1.9-MeV electron irradiation. The material-I was made using hot pressing (temperature 2150 °C, pressure 30 MPa, isothermal treatment for 15 min without protective atmosphere) the powders TiB_2 (54 mass.%) and TiC (46 mass.%).

The feature of the material-II was that 3 mass % B_4C was added to the above composition. In this case, as was shown in [6], titanium carbide and boron carbide were interacting in the course of hot pressing, with production of titanium diboride and release of carbon. The final composition of the material was formed in the course of synthesis according to the following reaction:

$$TiB_2 + TiC + xB_4C \rightarrow (1 + 2x)TiB_2 + (1 - 2x)TiC + xC.$$

Proceeding of this reaction made it possible to reduce the time of material compacting down to 8 min. It led to decreasing the average grain size as well as increasing microhardness and fracture toughness. It should be noted that metallographic analysis of materials-II made it possible to draw a conclusion about incomplete proceeding of the reaction: one can detect boron carbide inclusions (which content does not exceed 1%) at the specimen microsections.

The specimen geometry (tablets: 2-mm thick and 10-mm in diameter) was chosen due to efficient absorption of the electron flow. Electron irradiation was produced using a linear accelerator of charged particles "ИЛУ-6". The electron energy in the beam was 1.9 MeV, the average pulse current was 3 mA. In the course of irradiation, the temperature was maintained within the range 60 to 120 °C. The electron fluences were 10^{16}, 5×10^{16}, 10^{17}, 5×10^{17} and 10^{18} electron/cm^2 for specimens-I and specimens-II.

The phase composition of the specimens under investigation was determined with a diffractometer ДРОН-4 using copper radiation. The elemental composition was determined with a wave-dispersive spectrometer S8 TIGER (BRUKER ELEMENTAL). Microhardness and fracture toughness were measured using the Vickers technique with a DuraScan machine (EMCO-TEST Prüfmaschinen GmbH) in accordance with the procedures [7] and [8].

3. Experimental results and discussion

X-ray phase analysis found appearance of a graphite phase in specimens-I and specimens-II after electron irradiation (Table 1). This result may be related to structurization of X-ray amorphous carbon, either dissolved in the initial phases TiB_2 and TiC or released in the course of the chemical reaction $TiC + B_4C \rightarrow TiB_2 + C$ (in specimens-II). Similar structurization was detected on electron irradiation in amorphous materials [9]. The authors of [9] showed that the most probable mechanism of crystalline phase formation is the growth of pre-formed micrograins, while the electron flow serves predominantly for transportation. It is evident that a similar mechanism of phase formation was also observed in our case. Analysis of the fluence dependence of Ti, B and C concentrations (Fig. 1) also indicates the carbon transfer from the irradiated specimen side to the opposite (non-irradiated) one.

An analysis of the plots given in Fig. 2 shows that the mean microhardness values at the irradiated and opposite sides of the specimens having the same composition demonstrate the same character of the fluence dependence. Microhardness values at the opposite sides are lower than those at the irradiated ones. This fact may be explained by the transfer of carbon atoms to the non-irradiated specimen side (see also Fig. 1). Besides, the energy of electrons that reached the opposite side is below than that of the ones reaching the irradiated surface. According to the diffusion model, the energy E of electron that has passed a distance x in matter can be found from the expression [10]:

$$-\frac{dE}{dx} = \frac{E_0{}^n}{nRE^{n-1}} \text{ or } \frac{E}{E_0} = \sqrt{1 - x/R}. \qquad (2)$$

Table 1. Phase composition of the initial and irradiated specimens.

Specimen type	Fluence, electron/cm^2	Phase composition, %		
		TiB_2	TiC	C (graphite)
I	–	66	34	–
	10^{16}	68	32	–
	5×10^{16}	70	30	–
	10^{17}	67	31	2
	5×10^{17}	68	31	<1
	10^{18}	70	30	–
II	–	74	26	–
	10^{16}	75	25	–
	5×10^{16}	75	24	<1
	10^{17}	75	24	<1
	5×10^{17}	74	26	–
	10^{18}	74	24	2

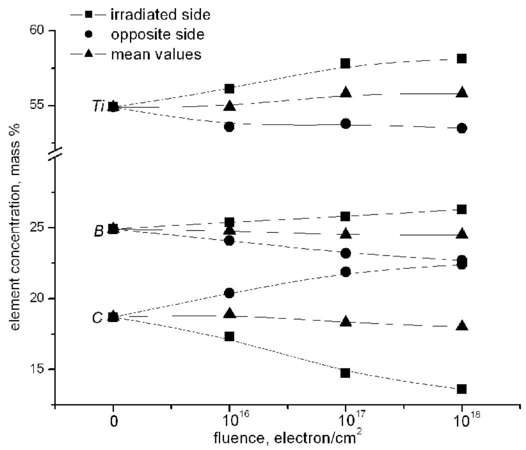

Fig. 1. Fluence dependence of Ti, B and C concentrations at the irradiated and opposite sides and their mean values for the specimen-I.

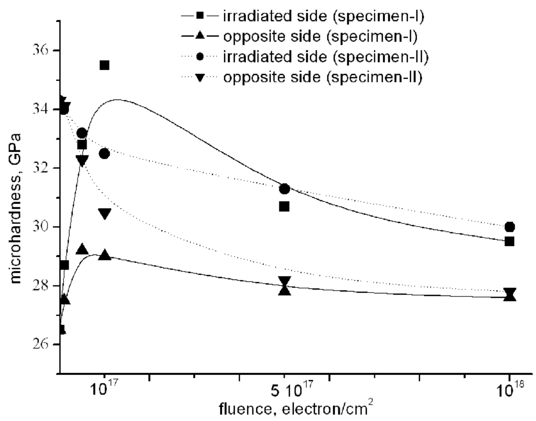

Fig. 2. Fluence dependence of microhardness for the specimen-I and specimen-II.

Here, E_0 is the initial electron energy, n – exponent in the generalized Thomson–Widdington law (in the classical approach, $n = 2$), R – electron range in the target:

$$R = \frac{2.76 \cdot 10^{-2} A E_0^{5/3}}{\rho Z^{8/9}} \cdot \frac{\left(1+0.978 \cdot 10^{-3} E_0\right)^{5/3}}{\left(1+1.975 \cdot 10^{-3} E_0\right)^{1/3}}, \qquad (3)$$

where Z is the atomic number, A – atomic weight, ρ – material density.

According to Eqs. (1, 2), reduction of the electron energy below the defect production threshold results in spending most of it for excitation of the atomic subsystem without producing defects. It leads to the enhancement of processes of radiation annealing. For our materials, the maximal energy of electron passed through the specimen (which thickness $x = 2$ mm) is ~1 MeV. Taking into account that the factual path of electrons exceeds the x value used in the calculation, we obtain that the probability of radiation defects production at the opposite specimen side decreases.

Table 2. Fluence dependence of fracture toughness (MPa·m$^{1/2}$).

Fluence, electron/cm^2	Specimen-I		Specimen-II	
	Irradiated side	Opposite side	Irradiated side	Opposite site
0	8.1±0.3	8.1±0.3	9.6±0.7	9.6±0.7
10^{16}	8.9±0.5	7.5±0.4	8.4±0.6	9.7±0.9
5×10^{16}	7.2±0.4	8.7±0.4	8.2±0.6	9.9±0.6
10^{17}	6.3±0.4	8.3±0.3	9.3±0.8	10.2±0.7
5×10^{17}	7.6±0.6	9.7±0.5	8.4±0.5	10.1±0.9
10^{18}	9.1±0.6	10.5±0.7	7.9±0.7	9.5±0.8

For specimens-I, a classical fluence dependence is observed on electron irradiation, namely, increase of microhardness followed by its reduction at a certain fluence value (in our case, 10^{17} electron/cm^2). The above behavior of microhardness is explained by accumulation of radiation defects. It leads to increase of intrinsic stresses (and, correspondingly, microhardness, yield strength and some other characteristics) and their partial annihilation due to increased interaction between neighboring defects (which is observed as reduction of microhardness).

For specimens-II, microhardness decreased over the whole fluence range. This qualitative distinction of the fluence dependence of microhardness is related to non-equilibrium of their phase composition acquired in the course of hot pressing. As a result, the specimens-II are inclined to electron radiation-induced phase transformations under irradiation, which compensate for microhardness increase caused by accumulation of radiation defects. At the fluence 5×10^{17} electron/cm^2 and higher, the average values of microhardness at the irradiated and opposite sides of specimens-I (specimens-II) have the same limit close to 30 GPa (~28 GPa).

Construction of microhardness distribution is more informative from the viewpoint of the investigation of structural-phase transformation of composite materials. Variation of phase composition, degree of perfection of boundaries between phases and other composite components leads to changes in microhardness distribution profiles [11, 12]. The initial microhardness distributions for the specimens-I and specimens-II (Figs 3.1 and 4.1) differ considerably because of distinctions in their microstructure.

It should be noted that, at the maximal irradiation fluences (Figs. 3.6 and 4.6), the microhardness distributions for the specimens-I and specimens-II have similar profiles at their irradiated (opposite) sides. Some distinctions between the distributions at the irradiated and opposite sides are related to (i) transport of carbon atoms along the direction of the electron current and (ii) different rate of radiation defects production at the corresponding surfaces.

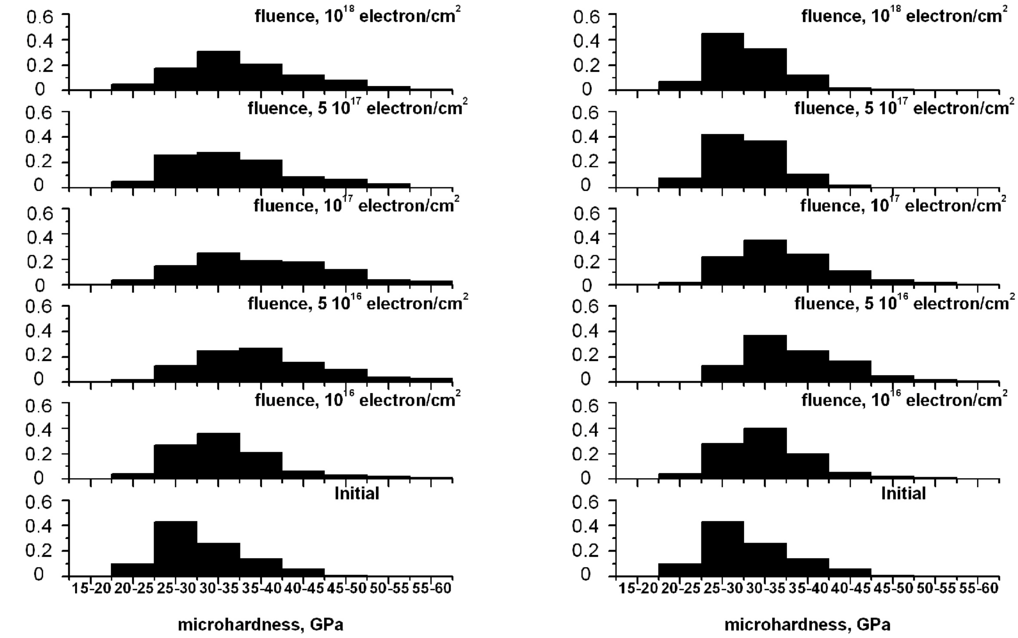

Fig. 3. Fluence dependence of microhardness distribution at the irradiated (left) and opposite (right) sides of the specimen-I. Fluence (electron/cm^2): 0 (*1*); 10^{16} (*2*); 5×10^{16} (*3*); 10^{17} (*4*); 5×10^{17} (*5*); 10^{18} (*6*).

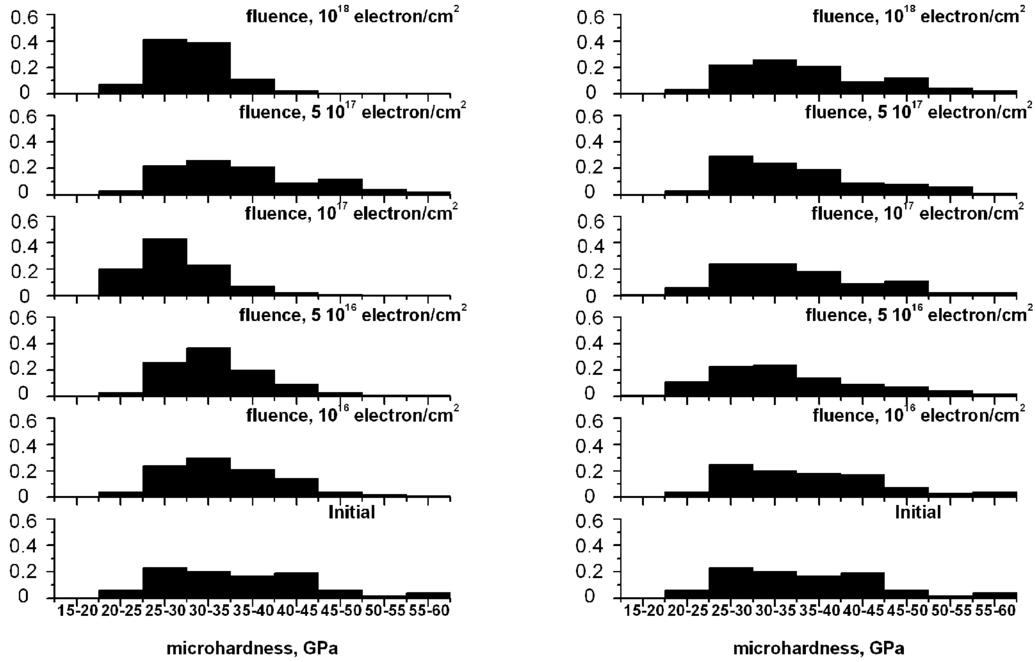

Fig. 4. Fluence dependence of microhardness distribution at the irradiated (left) and opposite (right) sides of the specimen-II. Fluence (electron/cm^2): 0 (*1*); 10^{16} (*2*); 5×10^{16} (*3*); 10^{17} (*4*); 5×10^{17} (*5*); 10^{18} (*6*).

The result obtained indicates transformation of both reactively-pressed and nonreactively-pressed specimens (exposed to electron irradiation) to similar structural-phase states despite their essentially different initial states. Higher microhardness values at the irradiated sides of the specimens-I and specimens-II are due to more intensive production of radiation defects.

4. Conclusions

We have demonstrated that electron irradiation of TiB_2–TiC materials leads to migration of carbon atoms from the irradiated specimen side to the opposite one.

The fluence dependences of microhardness distribution at the irradiated and opposite sides of the specimens-I and specimens-II are considerably different. The fracture toughness of the specimens under investigation (≈ 8 $MPa/m^{1/2}$) is rather high for ceramic materials, and its variation under electron irradiation does not exceed limits of errors.

The presence of the non-equilibrium phase component in specimens-II is a prerequisite to structural-phase transformations under the action of electron irradiation. It leads to stress relaxation and, consequently, can promote extension of material service life under irradiation.

References

1. V.D. Risovanyi, E.P. Klochkov, V.E. Ponomarenko, *Hafnium in Nuclear Engineering*. NIIR, Dimitrograd, 1993 (in Russian).
2. A.F. Grachev, V.N. Golovanov, V.D. Risovanyi, A.V. Zakharov et al., The prospects for development of absorbing materials and regulating units in Russia for 2000-2010, in: *Collected Reports of the 6-th Russian Conference on Reactor Materials Technology*, p. 83-127 (2001), in Russian.
3. D.R. Ni, L. Geng, J. Zhang, Z.Z. Zheng, Effect of B_4C particle size on microstructure of *in situ* titanium matrix composites prepared by reactive processing of Ti–B_4C system // *Scripta Materialia* **55**(5), p. 429-432 (2006).
4. D.R. Ni, L. Geng, J. Zhang, Z.Z. Zheng, TEM characterization of symbiosis structure of *in situ* TiC and TiB prepared by reactive processing of Ti–B_4C // *Materials Lett*. **62**(4-5), p. 686-688 (2008).
5. G.H. Kinchin, R.S. Pease, The displacement of atoms in solids by radiation // *Repts. Progress in Physics,* **18**(1), p. 1-51 (1955).
6. A.Yu. Popov, I.F. Kazo, V.A. Makara, S.V. Chornobuk, Structural-phase transformations in the course of synthesizing composite materials based on titanium and hafnium carbides and borides with superdispersed carbon inclusions // *Materialovedenie,* no 7, p. 54-56 (2007), in Russian.
7. V.K. Grigorovich, *Hardness and Microhardness of Metals*. Nauka, Moscow, 1976 (in Russian).
8. A.G. Evans, E.A. Charles, Fracture toughness determination by indentation // *J. Amer. Ceram. Soc*. **59**(7), p. 371-372 (1977).
9. V.Y. Povarchuk, V.B. Neimash, A.M. Kraitchynskii, V.V. Maslov, V.K. Nosenko, G.M. Zelins'ka, Effect of ionizing radiation on magnetic properties and structure of $Fe_{80}Si_6B_{14}$ amorphous alloy // *Ukr. J. Phys*. **49**(1), p. 90-93 (2004).
10. L.R. Minikaev, R.R. Tangishev, T.A. Kupriyanova, M.N. Filippov, M.A. Stepanovich, Estimation of range of kV electrons in a dielectric target with conducting coating at bulk charge accumulation, in: *XXI International Conference "Radiation Physics of Solids", Sevastopol, August 22-27, 2011*. FGBNU "NII PMT", Moscow, p. 252-256 (2011), in Russian.
11. I.M. Totsky, I.F. Kazo, O.Yu. Popov, V.A. Makara, Microhardness distribution in two-phase composite systems // *Visnyk Kyivs'kogo Universytetu, Ser. Fizyka i Matematyka,* no 2, p. 297-302 (2010), in Ukrainian.
12. V.V. Leonov, *Microhardness of One- and Two-Phase Alloys*, Mashinostroenie, Krasnoyarsk, 1990 (in Russian).